Near-field investigation of THz surface-wave emission from optically excited graphite flakes

M. Nagel,[1,*] A. Michalski,[1] T. Botzem,[1] and H. Kurz[1,2]

[1]*Institut für Halbleitertechnik, RWTH Aachen University, Sommerfeldstr. 24, 52074 Aachen, Germany*
[2]*AMO GmbH, Otto-Blumenthal-Straße 25, 52074 Aachen, Germany*
**nagel@iht.rwth-aachen.de*

Abstract: THz emission from an unbiased graphite flake after optical sub-ps pulse inter-band excitation is measured using a novel micro-machined photoconductive probe-tip. Oscillatory behavior of the measured THz near-field emission is shown to originate from electromagnetic eigenmode resonances of the laterally limited graphite flake. The excitation efficiency of the lowest order eigenmode resonances strongly dependents on optical pump location. From this data a radial symmetric charge carrier translocation at the pump location is revealed as the dominating THz surface-wave emission effect. Measurements show good agreement with numerical field simulations of the eigenmode center frequencies and the spectral response expected for THz emission through basal plane oriented radial current surge excitation.

OCIS codes: (300.6495) Terahertz spectroscopy; (040.2235) Far infrared or terahertz detectors; (320.7100) Ultrafast measurements.

References and links

1. F. Rana, "Graphene terahertz plasmon oscillators," IEEE Trans. NanoTechnol. **7**(1), 91–99 (2008).
2. V. Ryzhii, V. Mitin, M. Ryzhii, N. Ryabova, and T. Otsuji, "Device model for graphene nanoribbon phototransistor," Appl. Phys. Exp. **1**, 063002 (2008).
3. N. L. Rangel, and J. M. Seminario, "Graphene terahertz generators for molecular circuits and sensors," J. Phys. Chem. A **112**(51), 13699–13705 (2008).
4. V. Y. Aleshkin, A. A. Dubinov, and V. Ryzhii, "Terahertz laser based on optically pumped graphene: model and feasibility of realization," JETP Lett. **89**(2), 63–67 (2009).
5. M. Wächter, M. Nagel, and H. Kurz, "Tapered photoconductive terahertz field probe tip with subwavelength spatial resolution," Appl. Phys. Lett. **95**(4), 041112 (2009).
6. M. Awad, M. Nagel, and H. Kurz, "Tapered Sommerfeld wire terahertz near-field imaging," Appl. Phys. Lett. **94**(5), 051107 (2009).
7. J. M. Dawlaty, S. Shivaraman, M. Chandrashekhar, F. Rana, and M. G. Spencer, "Measurement of ultrafast carrier dynamics in epitaxial graphene," Appl. Phys. Lett. **92**(4), 042116 (2008).
8. R. W. Newson, J. Dean, B. Schmidt, and H. M. van Driel, "Ultrafast carrier kinetics in exfoliated graphene and thin graphite films," Opt. Express **17**(4), 2326–2333 (2009), http://www.opticsinfobase.org/abstract.cfm?URI=oe-17-4-2326.
9. M. Breusing, C. Ropers, and T. Elsaesser, "Ultrafast carrier dynamics in graphite," Phys. Rev. Lett. **102**(8), 086809 (2009).
10. P. A. George, J. Strait, J. Dawlaty, S. Shivaraman, M. Chandrashekhar, F. Rana, and M. G. Spencer, "Ultrafast optical-pump terahertz-probe spectroscopy of the carrier relaxation and recombination dynamics in epitaxial graphene," Nano Lett. **8**(12), 4248–4251 (2008).
11. T. Kampfrath, L. Perfetti, F. Schapper, C. Frischkorn, and M. Wolf, "Strongly coupled optical phonons in the ultrafast dynamics of the electronic energy and current relaxation in graphite," Phys. Rev. Lett. **95**(18), 187403 (2005).
12. H. Karasawa, T. Komori, T. Watanabe, A. Satou, H. Fukidome, M. Suemitsu, V. Ryzhii, and T. Otsuji, "Observation of amplified stimulated terahertz emission from optically pumped heteroepitaxial graphene-on-silicon materials," J. Infrared Millim. Terahz. Waves (2010), doi:10.1007/s10762-010-9677-1.
13. G. M. Mikheev, R. G. Zonov, A. N. Obraztsov, and Yu. P. Svirko, "Giant optical rectification effect in nanocarbon films," Appl. Phys. Lett. **84**(24), 4854 (2004).
14. J. M. Torres, "Nanosecond optical rectification and photon drag effect in nanocarbon thin films and wires," J. Nanoelectron. Optoelectron. **4**(2), 247–251 (2009).
15. G. Ramakrishnan, R. Chakkittakandy, and P. C. M. Planken, "Terahertz generation from graphite," Opt. Express **17**(18), 16092–16099 (2009), http://www.opticsinfobase.org/oe/abstract.cfm?URI=oe-17-18-16092.

#140007 - $15.00 USD Received 20 Dec 2010; revised 18 Feb 2011; accepted 18 Feb 2011; published 24 Feb 2011

16. D. Sun, C. Divin, J. Rioux, J. E. Sipe, C. Berger, W. A. de Heer, P. N. First, and T. B. Norris, "Coherent control of ballistic photocurrents in multilayer epitaxial graphene using quantum interference," Nano Lett. **10**(4), 1293–1296 (2010).
17. F. Carbone, P. Baum, P. Rudolf, and A. H. Zewail, "Structural preablation dynamics of graphite observed by ultrafast electron crystallography," Phys. Rev. Lett. **100**(3), 035501 (2008).
18. F. Carbone, "The interplay between structure and orbitals in the chemical bonding of graphite," Chem. Phys. Lett. **496**(4-6), 291–295 (2010).
19. J. Shan, and T. F. Heinz, in *Ultrafast Dynamical Processes in Semiconductors*, Topics in Applied Physics, K.-T. Tsen, ed., (Springer, 2004), Vol. 92, pp. 1–59.
20. M. Awad, M. Nagel, H. Kurz, J. Herfort, and K. Ploog, "Characterization of low temperature GaAs antenna array terahertz emitters," Appl. Phys. Lett. **91**(18), 181124 (2007).
21. L. G. Johnson, and G. Dresselhaus, "Optical properties of graphite," Phys. Rev. B **7**(6), 2275–2285 (1973).

1. Introduction

Many theoretical papers have highlighted the large potential of (multilayer) graphene or graphite materials for devices operating in the terahertz (THz) frequency range like plasmon oscillators [1], detectors [2], molecular sensors [3] or lasers [4]. However, the number of experimental THz-range investigations of graphitic materials or devices is still sparse. A lack of adequate THz measurement technology is a main reason for this discrepancy. Major deficits of common THz far-field radiation approaches are weak interaction of diffraction limited THz beams with sub-wavelength scale few atom-layer thick samples, insufficient spatial resolution as well as missing access to non-propagating electromagnetic modes. As demonstrated in this work, recent developments of highly sensitive THz near-field probing techniques can provide the urgently needed analytical access to THz range nanophotonic and nanoelectronic investigations [5,6].

Ultrafast carrier relaxation dynamics after inter-band excitation of epitaxial or exfoliated single and multilayer (ML) graphene flakes have been measured by near-infrared pump-probe spectroscopy [7–9]. Using optical pump/THz far-field probe spectroscopy carrier relaxation dynamics at lower energy levels were probe at large scale multilayer (ML) graphene samples epitaxially grown on SiC wafers [10] or exfoliated graphite samples [11]. Experimental investigation of THz emission of optically excited ML graphene is a phenomenon addressed only recently by first groups: Large-scale epitaxial ML graphene samples were investigated by Karasawa et al. using an electro-optic near-field probing configuration [12]. The measured signals were interpreted as stimulated terahertz emission from the ML graphene sample. Unfortunately, other optically induced THz generation mechanisms with probably higher relevance – especially photocurrent related ones – where not considered in this work. Possible alternative mechanisms are optical rectification (based on quadrupole optical nonlinearity) [13] or photon-drag effects (based on momentum transfer between photons and free charge carriers) which where both studied at graphite-based nanocrystalline films using nanosecond near-infrared pulse excitation [14]. These effects have also been discussed as possible THz generation mechanisms in case of sub-ps pulse excitation. However, experimental verification is lacking so far.

A first demonstration of photo-current induced THz generation at bulk graphite surfaces excited by sub-ps near-infrared pulses was recently given by Ramakrishnan et al. [15]: Magnetic-field induced enhancement of THz emission distinctly showed that a transient movement of optically excited charge carriers is responsible for THz emission from bulk graphite. Later, Sun et al. [16] demonstrated that unidirectional THz emitting photo-currents can also be purely optically injected and controlled in ML graphene using quantum interference of one- and two-photon absorption processes. However, characteristic and reason of charge movement in the simple unbiased case of one-photon inter-band absorption is still giving rise to speculations. In [15] it was concluded that THz far-field emission from the optically excited basal plane surface of bulk graphite is most likely created by transient charge movement in a direction normal to the graphene planes. However, conductivity in this direction is more than three orders of magnitude lower than along the graphene planes. Previous ultrafast electron diffraction measurements revealed the tendency of c-axis chemical bonds in graphite to be destabilized by the photo-induced coherent motion of ions leading to

#140007 - $15.00 USD Received 20 Dec 2010; revised 18 Feb 2011; accepted 18 Feb 2011; published 24 Feb 2011

crystal compression in normal direction to the basal planes [17]. It was recently suspected, that the charge flow induced by this c-axis compression could also be responsible for the emission of THz radiation observed by Ramakrishnan et al. [18].

In this work, continuative experimental and theoretical investigations on THz emission from an optically excited exfoliated graphite flake are presented. We introduce a photoconductive near-field probe configuration able to measure the THz near-field emission directly at the flake. In contrast to earlier near-field measurements [12] THz background emission from the probe itself is avoided. Opposed to far-field configurations our near-field probe is able to detect the non-radiated THz fields generated in the case of normal incidence of the optical excitation beam. Our results reveal a previously not considered possibly essential importance of basal plane directed carrier transport for the THz emission process.

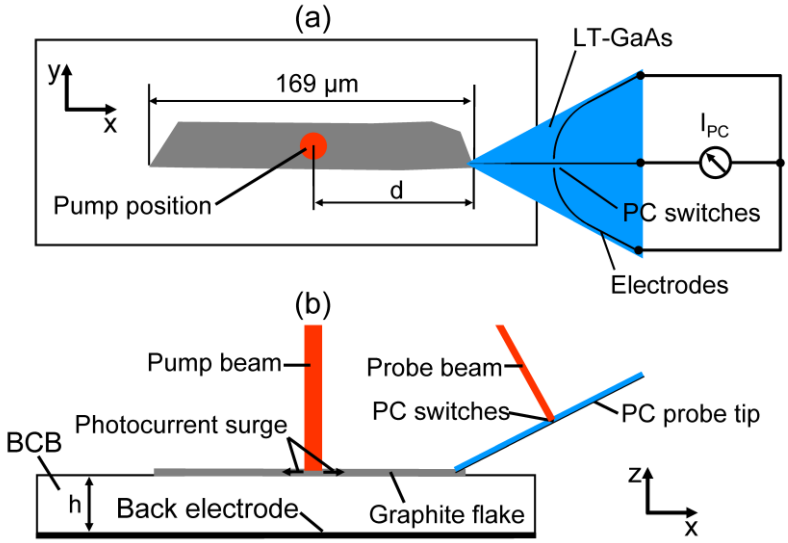

Fig. 1. (a) Top-view of the PC probe-tip structure. (b) Cross-section of the applied sample structure and pump/probe configuration.

2. Experimental setup

Generation of current surge at optically excited semiconductor surfaces or lateral metal-semiconductor-metal (MSM) structures is among the most popular effects used for the induction of pulsed THz radiation [19]. Under certain configurations – even in the presence of a local surface current surge – THz far-field radiation is not observed, e.g. if the charge movement and the direction of excitation/observation are both parallel to the surface normal or if the sum of multidirectional transversal current densities cancels out [20]. Both effects can be responsible for the absence of THz far-field emission from a surface or planar structure under normal incidence, as recently also observed at the graphite basal plane surface [15]. Using near-field probing, however, it is still possible in such a case to detect the generated (but not radiated) THz field close to the position of optical excitation.

The photoconductive (PC) probe-tip, the sample shape and configuration used in this study are schematically sketched in Fig. 1(a) in top-view and in Fig. 1(b) in cross-section. The probe-tip is based on a 1.3 µm thick free-standing triangular shaped low-temperature-grown (LT-) GaAs cantilever featuring planar Cr/Au electrode structures. The fabrication process has been described elsewhere [5]. An important difference to the earlier design [5] is that the probe-tip is sensitive to THz-field components in axial direction as opposed to horizontal components. It is equipped with a planar tapered single-wire electrode with a tip-radius of approx. 200 nm. Axial field components are coupled to the tip and transmitted over the single-wire as radial quasi-Sommerfeld modes [6], just slightly degenerated by the ultra-thin

#140007 - $15.00 USD Received 20 Dec 2010; revised 18 Feb 2011; accepted 18 Feb 2011; published 24 Feb 2011

(~lambda/260) dielectric LT-GaAs support. The transmitted radial mode is sampled by a pair of PC switches. The sensitivity of both PC switches is balanced by matching the photo-current of the illuminated switches prior to the measurement.

The sample is fabricated using the following steps: First, a 40-µm-thick layer of bencocyclobutene (BCB) is spin-coated and thermally cured on a Ti/Au layer (10 nm/200 nm) on top of a silicon substrate. A graphite flake with a length and width of 169 µm and 26 µm, respectively, is deposited on top of the BCB surface via exfoliation of highly oriented pyrolytic graphite (HOPG) bulk material. Using an atomic force microscope (AFM) the flake thickness is determined as 130 nm. For the experiment the graphite flake is excited under normal incidence by optical pump pulses from a Ti:Sapphire laser with a center wavelength of 780 nm, 150 fs pulse width (FWHM), 78 MHz repetition rate and linear polarization. The average pump power is 44 mW and the excitation focus diameter is approximately 20 µm. The corresponding excitation fluence is 0.18 mJ/cm^2. The optical penetration depth δ of HOPG at 780 nm is 20 nm [21]. The flexible PC probe tip is brought into contact with the graphite flake surface in a position close to the edge (as shown in Fig. 1(b)) where the generated THz signals are coupled to the tip. The picked-up electric field signals E_{THz} (t) are sampled at the pair of PC switches by temporally delayed optical probe pulses taken from the same laser source using a beam splitter. The measured time-delay-dependent photocurrent I_{PC}(t) is proportional to E_{THz} (t).

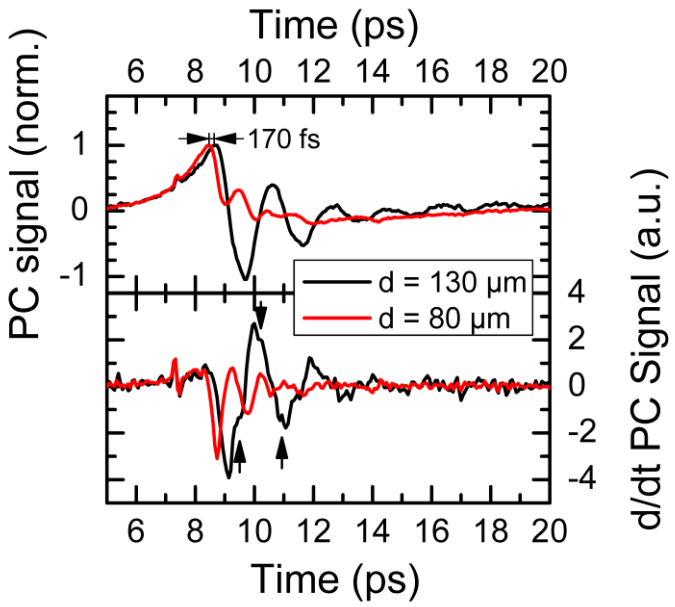

Fig. 2. (Upper diagram) Time-domain data of the optically generated field pulses at the graphite flake measured in pump/probe-tip distances d = 130 µm (black line) and 80 µm (red line). (Lower diagram) Time-derivative of the upper time-domain data.

3. Measurement and simulation results

Time-domain signals measured at the graphite flake for pump/probe position distances d = 130 µm and 80 µm are plotted in the upper diagram of Fig. 2. Both field pulses are characterized by an initial slow increase followed by a decaying field oscillation with period durations of 1 ps and 2 ps, for the near-center (NC) (d = 80 µm) and the off-center (OC) pump position (d = 130 µm), respectively. The peak of the THz signal generated in shorter probe-tip distance arrives 170 fs earlier than the peak of the second signal travelling a 50 µm longer distance. It is deduced that the velocity of the initially generated wave equals approximately the speed of light. Since the optical penetration depth is less than a sixth of the flake thickness

#140007 - $15.00 USD Received 20 Dec 2010; revised 18 Feb 2011; accepted 18 Feb 2011; published 24 Feb 2011

the initially induced THz wave is obviously effectively screened from the polymer substrate. Consequently, it is able to propagate almost at light-speed as a surface plasmon polariton wave along the semimetal/air interface without substrate-induced dielectric retardation.

The two-fold oscillation speed observed for NC excitation compared to the OC excitation clearly indicates that surface-waves starting from the location of optical excitation are propagating in positive and negative x-direction along the flake. In the case of OC excitation the wave being reflected from the open end of the graphite flake (shortly after optical excitation) interferes constructively with the un-reflected wave already propagating in positive x-direction. The presence of two superimposed pulses propagating unidirectional in short spatio-temporal distance is clearly visible in the time-derivative data in the lower diagram of Fig. 2 where small dips (marked by arrows) appear close to the local peaks of the PC signal. In contrast, for NC excitation no dips are observed due to the almost permanent lack of unidirectional propagation.

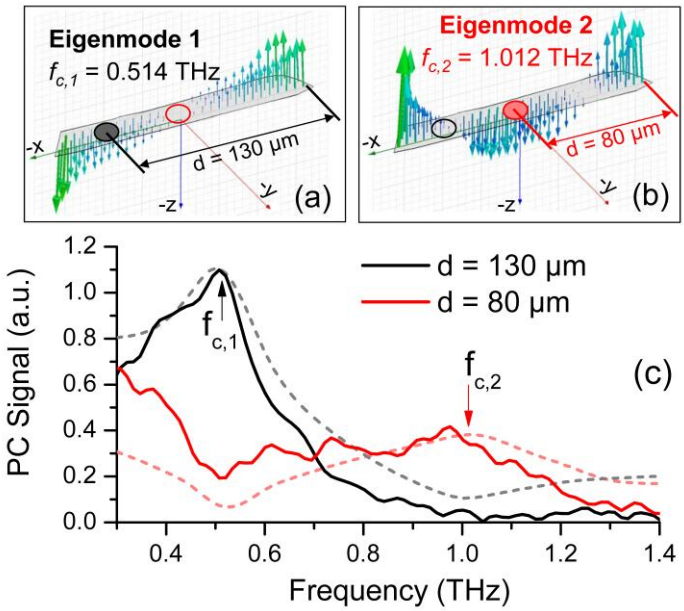

Fig. 3. Numerical calculation of the vectorial electric field distribution at the graphite flake surface for (a) the first- and (b) the second-order eigenmode resonance. (c) Measured (continuous line) and calculated (dashed line) field amplitude spectra obtained by near-field probing. The spectral positions of the calculated eigenmodes center frequencies are marked by arrows.

In order to study the origin of the oscillatory response in more detail, eigenmode (EM) resonances of the investigated graphite flake are calculated using HFSS (Version 12.1) from Ansoft which is a Maxwell equation solver based on the finite-element-method. The constructed 3D model accounts for the exact lateral shape of the flake. Furthermore, the model is taking into account the thickness (40 µm) and permittivity (ε_r = 2.7) of the BCB layer as well as the finite conductivity of the back-electrode ($\sigma_{Au} = 4.1 \cdot 10^7$ S/m). The graphite flake is approximated as metallic sheet with finite conductivity ($\sigma_{HOPG,basal\ plane} = 2.5 \cdot 10^6$ S/m) and zero-thickness. The presence of the probe-tip is intentionally not included in this model.

The obtained electric field vector distributions of the two lowest-order EMs of the investigated flake at the air/graphite interface are depicted in the inlay plots (a) and (b) of Fig. 3. The resonance frequencies of the calculated EMs are $f_{r,1}$ = 0.514 THz and $f_{r,2}$ = 1.012 THz. Exemplary assumption of vacuum permittivity ε_r = 1 for the BCB substrate layer yields strongly blue-shifted EM resonance frequencies $f_{r,1,vac}$ = 0.69 THz and $f_{r,2,vac}$ = 1.62 THz. The calculated EM resonance frequencies $f_{r,n}$ (n = 1,2) as marked by the position of the black and

#140007 - $15.00 USD Received 20 Dec 2010; revised 18 Feb 2011; accepted 18 Feb 2011; published 24 Feb 2011

red arrows in Fig. 3(c) show excellent agreement with the measured resonance frequencies given by the amplitude peak positions within the plotted spectra (represented by the continuous lines) which are obtained from the time-domain signals of Fig. 2 using Fourier-transformation. This result proves that the invasiveness of the probe-tip is very low because resonance frequency shifts introduced by the probe are negligible.

The spectral data in Fig. 3(c) further show that both pump positions match selectively with either a field node area of the first or the second-order EM (see Figs. 3(a) and 3(b)). The EM with a congruent field-node/pump area (represented by an open circular area) is not excited, while EM excitation is observed in the non-congruent cases (represented by a filled circular area). Further investigations with oblique incidence exhibited unchanged spectral response but decreased THz field amplitude. Only small dependencies to the polarization angle of the pump beam are observed for normal and oblique incidence. We can therefore exclude optical rectification and photon-drag effect as dominant THz generation mechanisms for the given case. Since the observed THz emission is generated without the presence of a second external THz stimulation source we can also exclude stimulated radiative electron-hole recombination as a self-sufficient generation process. All together, these results lead to the conclusion that an optically induced current surge with radial symmetry to the center of the excitation spot is responsible for THz pulse induction. Based on the present results we can, however, not yet unambiguously determine whether this charge movement is of vertical or radial nature or a sequential process of both.

To clarify the nature of charge movement, we extended our theoretical model by including a current source excitation and an electromagnetic model of the attached probe-tip. Within the full area of optical excitation a radial current source was approximated by four slices of orthogonally directed in-plane and in-phase current sources. The simulated spectral evolution of the generated field amplitude transmitted to the PC switch position of the probe-tip is shown for both excitation positions in Fig. 3(c) by the dashed curves. Very good agreement between experimental and simulated data is achieved for both pump positions. In order to achieve similar good agreement under assumption of a vertical dipole oscillation the excitation focus diameter had to be reduced to unreasonable 2 µm. These results are a first hint that radial in-plane currents dominate the THz emission process. Additional simulations of a non-contact configuration confirmed that the main influence of the probe is a spectral broadening of the resonance (equivalent to faster amplitude decay in time-domain).

4. Conclusion and outlook

In conclusion we have demonstrated first measurements of THz emission from unbiased singular graphite flakes after one-photon inter-band excitation. Specific orders of electromagnetic eigenmode resonances of the graphite flakes were selectively excited by pump position variation from which radial symmetric movement of optically excited charge carriers was identified as the dominating THz emission effect. These investigations were enabled by novel micro-machined photo-conductive probe-tips permitting highly sensitive low-invasive measurements of THz near-field emission directly at the surface of graphite flakes. Next experiments will be targeted on the spatio-temporal resolved vectorial mapping of photo-induced charge movement and THz emission within the direct area of optical excitation at thinner few-layer graphene samples and backside illumination.

Acknowledgments

The authors gratefully acknowledge financial support by the Deutsche Forschungsgemeinschaft (DFG) in frame of the project “Ultragraphen.” We also thank Prof. P. Planken for helpful discussion.

#140007 - $15.00 USD Received 20 Dec 2010; revised 18 Feb 2011; accepted 18 Feb 2011; published 24 Feb 2011